

Non-destructive imaging of internal structures of a mosquito with sub-micrometer resolution

Georg Schulz^{a,b}, Elena Spörri^{c,d}, Martin Gschwind^{c,d}, Hans Deyhle^b, and Bert Müller^b

^aCore Facility Micro- and Nanotomography, Department of Biomedical Engineering, University of Basel, Hegenheimermattweg 167 C, 4123, Allschwil, Switzerland

^bBiomaterials Science Center, Department of Biomedical Engineering, University of Basel, Hegenheimermattweg 167 C, 4123, Allschwil, Switzerland

^cSwiss Tropical and Public Health Institute, Kreuzstrasse 2, 4123, Allschwil, Switzerland

^dUniversity of Basel, Petersplatz 1, 4001, Basel, Switzerland

ABSTRACT

Inline X-ray phase tomography has emerged as one of the most suitable imaging techniques for the three-dimensional examination of soft tissue at the microscopic level. Historically, this method was constrained to synchrotron radiation due to its specific requirements, such as beam coherence. However, recent advancements in detector technology (optical magnification) and X-ray sources (e.g., smaller source sizes and liquid metal sources) have enabled the transfer of this technology to laboratory settings. In this study, we investigated selected parts of an ethanol-fixated mosquito—specifically the head, abdomen, and proboscis—at the sub-cellular level using the Xradia 610 Versa (Carl Zeiss X-ray Microscopy, Inc., Dublin, California, United States) with voxel sizes as small as 180 nm. A single lens of the compound eye was segmented from the data set of the head, and the focal length was calculated to be 22 μm . These results demonstrate the capability of laboratory-based X-ray phase tomography for high-resolution imaging of soft tissues, facilitating detailed structural analyses previously achievable only with synchrotron radiation.

Keywords: Mosquito, X-ray microtomography, laboratory-based tomography, optical magnification

1. INTRODUCTION

Understanding the intricate morphology of mosquitoes is crucial for advancements in entomological research [1–3], vector control strategies [4], and disease transmission studies [5, 6]. Traditionally, high-resolution imaging techniques like electron microscopy (EM) have been the gold standard for studying mosquito structures [7, 8], particularly when surface details are required at the nanoscale. Scanning electron microscopy (SEM), for example, provides exceptionally detailed images of external features, revealing the complex surface topology of mosquitoes with remarkable clarity [9–12]. However, electron microscopy is fundamentally limited to surface imaging or thin sections, making it challenging to investigate internal structures in a non-destructive manner.

So far the highest spatial resolutions for imaging insects were obtained by synchrotron radiation-based microtomography (SR micro-CT) [13–15]. Laboratory-based microtomography (micro-CT) was limited to a spatial resolution of 1–2 μm [16]. Recent advances in X-ray micro-CT offer an alternative that complements and extends the capabilities of electron microscopy and SR micro-CT. With isotropic resolutions of laboratory systems reaching down to 500 nm, microtomography can produce 3D renderings of biological specimens that are visually comparable to those obtained via electron microscopy. Yet, micro-CT provides a distinct advantage by enabling the non-invasive visualization of both surface and internal structures simultaneously. This ability to capture the mosquito's exoskeleton alongside internal tissues, such as the brain, stomach, and other organ systems, offers a more comprehensive view of its anatomy.

Optical coherence tomography (OCT) has also been explored as a non-invasive imaging technique for biological samples, including insects. A study employing OCT to image a mosquito demonstrated the ability to

Send correspondence to G.S.: e-mail: georg.schulz@unibas.ch, Phone: +41 61 207 5437

visualize internal features [17], though at a lower resolution compared to micro-CT. While OCT provides valuable internal imaging capabilities and offers rapid, non-destructive scanning, its resolution is generally in the range of a few microns, which limits the detailed surface and internal feature resolution achievable. In contrast, micro-CT at 500 nm offers significantly finer detail, providing both surface and volumetric data with higher fidelity. The comparison between these two non-invasive techniques highlights the distinct advantage of micro-CT for achieving sub-micron resolution and capturing both external and internal structures in a single scan.

The application of microtomography to mosquito imaging presents possibilities for detailed 3D reconstructions of entire organisms without the need for physical sectioning. It bridges the gap between high-resolution surface imaging and volumetric internal analysis, making it an invaluable tool for exploring both morphological features and functional anatomy. By comparing the results of micro-CT imaging to traditional electron microscopy, we can appreciate the advantages each technique offers while acknowledging the expanded insights provided by microtomography's ability to uncover internal complexities with unprecedented clarity.

In this study, we demonstrate the use of micro-CT to achieve an isotropic resolution of 500 nm in imaging a mosquito, highlighting both the surface and internal structures with 3D visualization. This resolution represents a significant improvement in capturing fine morphological details in a single non-destructive scan, offering a comprehensive approach to mosquito anatomy and structure-function relationships.

2. MATERIALS AND METHODS

For the microtomographic acquisition, the mosquito was immersed in a container with 100% ethanol (see Fig. 1 top). An Xradia 610 Versa (Carl Zeiss X-ray Microscopy, Inc., Dublin, California, United States) was used. The system is equipped with a 25 W X-ray tube with a maximal acceleration voltage of 160 kV. The detection

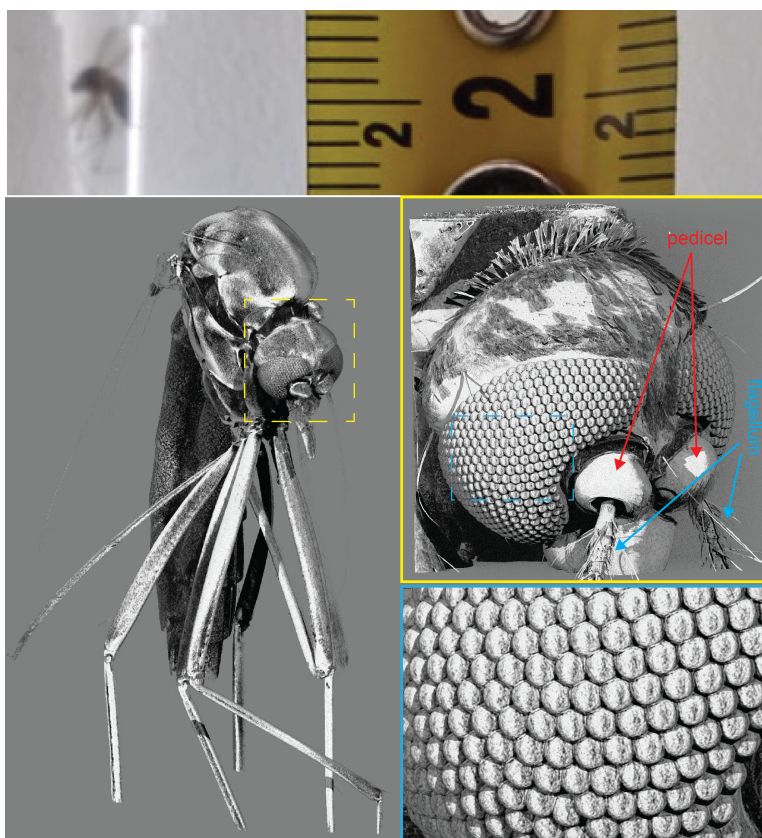


Figure 1. The top image shows the mosquito immersed in ethanol for microtomography. 3D rendering of a mosquito with zoom-ins on the head and eye, showing individual facets of the compound eye.

system is equipped with a 4 MegaPixel CCD, a 0.4× objective for overview scans and a turret containing three objectives (4×, 20×, 40×) for optical magnification. Each objective features an optimized scintillator. After an overview scan of the entire mosquito with the 4× objective, the head and abdomen of the mosquito were scanned with the 20× objective. For the highest spatial resolution, the 40× objective was used for the visualization of the proboscis. The settings of the scans can be found in Table 1.

Table 1. Scanning parameters.

	voltage [kV]	current [μA]	pixel size [μm]	exp. time [s]	# projections
entire mosquito	40	75	2.4	6	1601
mosquito head	50	90	0.38	13	3001
mosquito abdomen	50	90	0.36	10	3601
proboscis	50	90	0.18	26	5601

3. RESULTS AND DISCUSSION

Before the acquisition of the individual organs of the mosquito, an overview of the entire insect was performed. Fig. 1 left shows a 3D rendering of the entire animal. Due to the spatial resolution of around 3 μm , some features such as the wings and the proboscis are missing in the illustration. This data set was then used to align the object for the high-resolution scan of the head. The data set allows the identification of the pedicels, which are the donut-shaped structures, and which receive vibratory signals from the flagella (see Fig. 1 right top). A zoom on the eye of the mosquito (Fig. 1 right bottom) impressively shows the individual facets in a similar fashion as electron microscopy.

In order to visualize the inner structures of the head, it was essential to carry out the measurements in ethanol. For the first measurements, the mosquito was scanned fresh in the air. Although the external shape was well restored, the internal structures were deformed, sometimes even missing. These artifacts were caused by the drying of the specimen. Fig. 2 top shows virtual sections through the head of the mosquito including

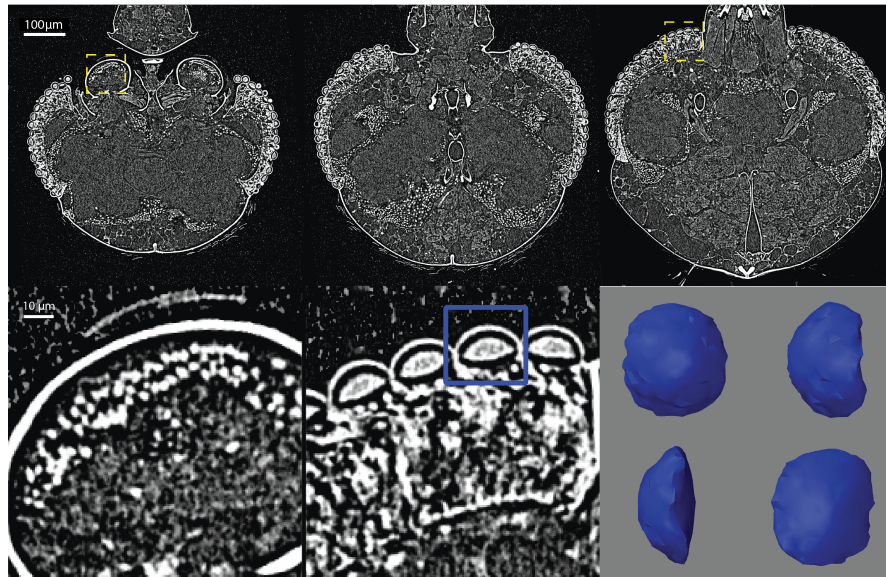


Figure 2. Virtual slices through the head of the mosquito (top row). The zoom-ins (bottom row) indicate individual neurosensory cells within the pedicel (left) and individual lenses and photoreceptors of the facets. Bottom right are 3D renderings of a selected lens from different views after segmentation.

the brain at the subcellular level. The two zoomed images below show individual neurosensory cells within the pedicel (left) and individual lenses and photoreceptors of the facets. Fig. 2 bottom right shows a 3D rendering of a selected segmented lens which was used for calculations of the focal length. For the calculation of the focal length f the modified Lensmaker's Equation when with a lens placed between two different media:

$$\frac{1}{f} = \frac{n_2 - n_1}{R_1} - \frac{n_2 - n_3}{R_2}, \quad (1)$$

with $n_1 = 1$ being the refractive index of air, $n_2 = 1.43$ of the mosquito lens [18] and $n_3 = 1.34$ of the medium behind the lens [19]. $R_1 \approx 10 \mu\text{m}$ and $R_2 \approx 24 \mu\text{m}$ are the two estimated radii of curvature as shown in Fig. 3. For the calculation of the focal length of a double-convex lens, R_2 has a negative sign. Using these values, the calculation results in a focal length of about $22 \mu\text{m}$. Although the thickness of the lens with about $9 \mu\text{m}$ is not negligible small with respect to R_1 , there is no need to use the thick lens formula, as the last expression of the formula is negligible due to the small difference between n_2 and n_3 . Looking inside the facet in the tomographic data set, this value for the focal length seems to be reasonable. The calculated focal length was determined using a randomly selected lens. In a future study, we plan to examine all facets of the compound eyes (about 500 per mosquito) to obtain statistics and analyze possible variations in focal length depending on the position of the facet. The study will use quantitative data from SR micro-CT to validate the refractive indices of the lens and the tissue behind the lens. These data are also used to quantify lens deformations and to determine the change in the refractive index of the lens and the tissue behind it caused by ethanol dehydration.

After the acquisition of the head, the mosquito was aligned to capture the abdomen. This region is very important for the life cycle of malaria parasites, as they eventually migrate to the liver and the midgut wall [21]. The three orthogonal slices in Fig. 4 show the stomach of the mosquito with a cellular resolution.

With a diameter below $100 \mu\text{m}$ the proboscis of the mosquito was visualized with the highest objective available (40x) resulting in a pixel size of 180 nm . A 3D rendering of it is shown in Vid. 1. The labium is the outer covering of the proboscis. This sheath folds back when the proboscis penetrates the victim's flesh. The two labella at the end of the proboscis are sensory organs that help the mosquito to find a good place to bite. When the Labium folds back, six tools appear that are essential for the mosquito bite. The structures are illustrated in the schematic in Fig. 5 left. The labrum acts as probe, which searches for blood vessels and at the end sucks the blood. The two maxillae (Mx) are used to saw through the skin, whereas the two Mandibles (M) are holding the tissue apart. The hypopharynx (H) could be thought as the tongue of the mosquito. The three virtual sections through the proboscis show the internal structure including the labrum and the maxillae.

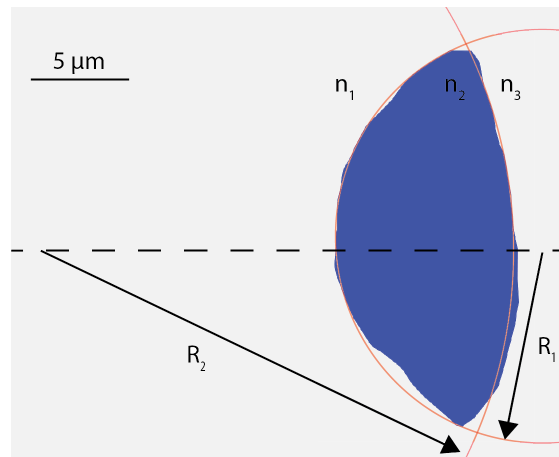


Figure 3. Schematic for calculation of the focal length of the segmented mosquito lens (blue).

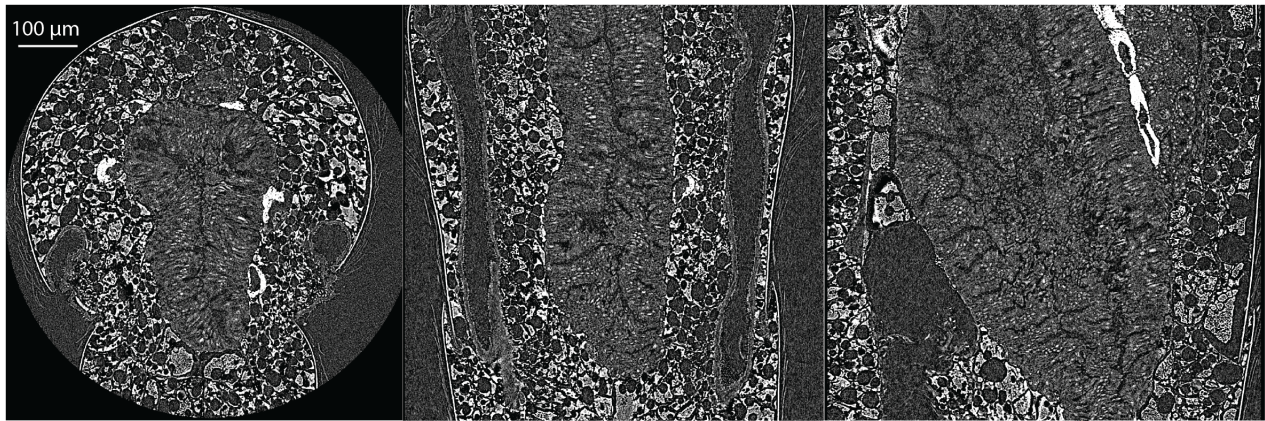


Figure 4. Orthogonal slices through the abdomen of a mosquito.

4. CONCLUSIONS

This study demonstrates the power of X-ray phase tomography for non-destructive, high-resolution imaging of complex biological samples, specifically focusing on a mosquito. The combination of whole-body 3D renderings at lower resolutions and high-resolution scans of individual organs, such as the head and proboscis, reveals detailed morphological features comparable to those achieved with electron microscopy, but with the additional ability to visualize internal structures. The challenges of preserving internal structures were evident in the early scans performed with the mosquito in air, where dehydration led to significant artifacts. By using ethanol as a medium, internal structures, including neurons in the pedicel and photoreceptors in the compound eye, were well-preserved and clearly visualized in the sub-cellular tomography. The calculation of the focal length of a single lens within the compound eye, based on the modified Lensmaker's equation, further highlights the precision achievable with this technique. The imaging of the proboscis demonstrated the versatility of micro-CT to capture fine anatomical details such as the labrum, maxillae, Mandibles, and hypopharynx, which are critical to the mosquito's feeding process. This ability to image and segment structures as small as the mosquito's proboscis at voxel sizes down to 180 nm represents a significant step forward in entomological research, enabling unprecedented insight into both surface and internal anatomy without destructive sectioning.



Video 1. 3D rendering of the proboscis with the surface of the labium. <http://dx.doi.org/10.1117/12.3029450.1>

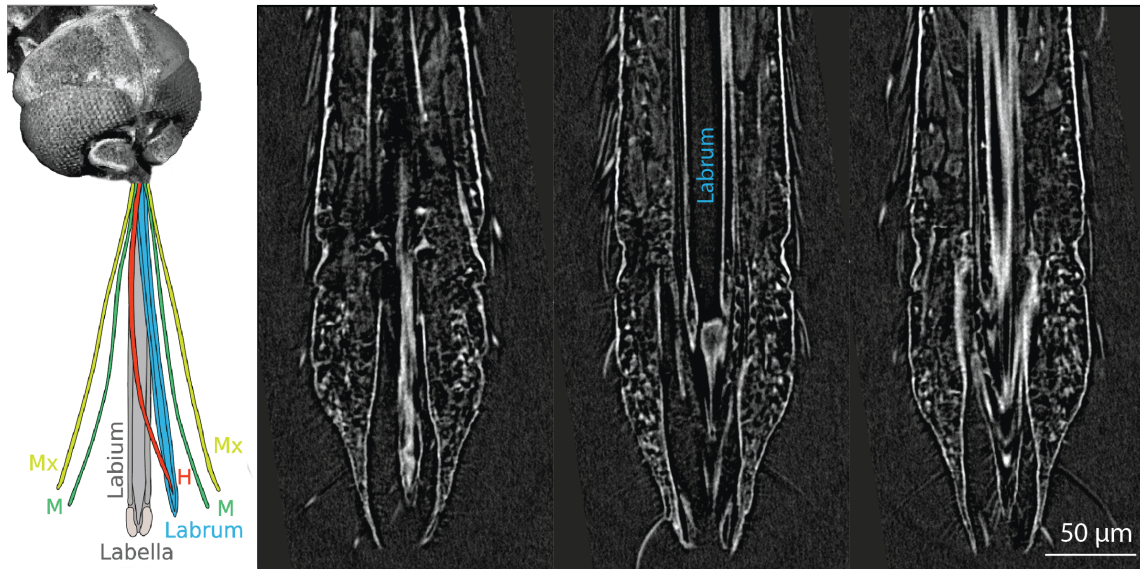


Figure 5. Schematic representation of the internal features of the proboscis (left) inspired by illustration in [20] and a series of virtual slices through the microtomography dataset.

The study illustrates the capabilities of laboratory-based microtomography for detailed 3D structural analysis at the sub-micron level. The technique not only rivals electron microscopy in terms of surface visualization but also surpasses it by uncovering internal structures critical for understanding mosquito anatomy and function. The findings open avenues for high-resolution imaging in entomology and could be instrumental for studying the life cycle of parasites and other internal biological processes in mosquitoes, with potential applications for disease control and vector biology.

ACKNOWLEDGMENTS

The authors acknowledge financial support of the Swiss National Science Foundation (SNSF) in the frame of the R²Equip initiative (316030.205646) and support from the mosquito breeding facility at the Swiss TPH.

REFERENCES

- [1] Cordeiro Rocha, V. and Ferreira Martins, G., “Midgut morphology of the predator mosquito *lutzia bigoti* (diptera: Culicidae) and its implications for feeding behavior,” *Acta Tropica* **257**, 107289 (2024).
- [2] Wiegmann, B. M., Trautwein, M. D., Winkler, I. S., Barr, N. B., Kim, J.-W., Lambkin, C., Bertone, M. A., Cassel, B. K., Bayless, K. M., Heimberg, A. M., Wheeler, B. M., Peterson, K. J., Pape, T., Sinclair, B. J., Skevington, J. H., Blagoderov, V., Caravas, J., Kutty, S. N., Schmidt-Ott, U., Kampmeier, G. E., Thompson, F. C., Grimaldi, D. A., Beckenbach, A. T., Courtney, G. W., Friedrich, M., Meier, R., and Yeates, D. K., “Episodic radiations in the fly tree of life,” *Proceedings of the National Academy of Sciences* **108**(14), 5690–5695 (2011).
- [3] Reinert, J. F., Harbach, R. E., and Kitching, I. J., “Phylogeny and classification of Aedini (Diptera: Culicidae), based on morphological characters of all life stages,” *Zoological Journal of the Linnean Society* **142**, 289–368 (11 2004).
- [4] Gupta, K. A., Ikonomidou, V. N., Glancey, M., Faiman, R., Talafha, S., Ford, T., Jenkins, T., and Goodwin, A., “Mosquito species identification accuracy of early deployed algorithms in idx, a vector identification tool,” *Acta Tropica* **260**, 107392 (2024).
- [5] Wells, M. B., Villamor, J., and Andrew, D. J., “Salivary gland maturation and duct formation in the african malaria mosquito *anopheles gambiae*,” *Scientific Reports* **7**, 601 (2017).

- [6] Pala, Z. R., Alves e Silva, T. L., Minai, M., Crews, B., Patino-Martinez, E., Carmona-Rivera, C., Valenzuela Leon, P. C., Martin-Martin, I., Flores-Garcia, Y., Cachau, R. E., Muslinkina, L., Gittis, A. G., Srivastava, N., Garboczi, D. N., Alves, D. A., Kaplan, M. J., Fischer, E., Calvo, E., and Vega-Rodriguez, J., “Mosquito salivary apyrase regulates blood meal hemostasis and facilitates malaria parasite transmission,” *Nature Communications* **15**, 8194 (2024).
- [7] Kantor, A. M., Grant, D. G., Balaraman, V., White, T. A., and Franz, A. W. E., “Ultrastructural analysis of chikungunya virus dissemination from the midgut of the yellow fever mosquito, *aedes aegypti*,” *Viruses* **10**(10) (2018).
- [8] Martins, G. F., Ramalho-Ortigão, J. M., and Pimenta, P. F. P., “Morphological features of the heart of six mosquito species as revealed by scanning electron microscopy,” *International Journal of Tropical Insect Science* **31**(1–2), 98–102 (2011).
- [9] Kong, X. Q. and Wu, C. W., “Mosquito proboscis: An elegant biomicroelectromechanical system,” *Phys. Rev. E* **82**, 011910 (Jul 2010).
- [10] Amer, A. and H., M., “The sensilla of *aedes* and *anopheles* mosquitoes and their importance in repellency,” *Parasitology Research* **99**, 491–499 (2006).
- [11] Gibson, W., Peacock, L., and Hutchinson, R., “Microarchitecture of the tsetse fly proboscis,” *Parasites Vectors* **10**, 430 (2017).
- [12] Albergaria, R. G., dos Santos Araújo, R., and Martins, G. F., “Morphological characterization of antennal sensilla in *toxorhynchites theobaldi*, *toxorhynchites violaceus*, and *lutzia bigoti* adults: a comparative study using scanning electron microscopy,” *Protoplasma* **261**, 671–684 (2024).
- [13] Ha, Y.-R., Lee, S.-C., Seo, S.-J., Ryu, J., Lee, D.-K., and Lee, S.-J., “Comparison of the functional features of the pump organs of *anopheles sinensis* and *aedes togoi*,” *Scientific Reports* **5**, 15148 (2015).
- [14] Vilhelmsen, L., Boudinot, B., Shaw, J. J., Hammel, J. U., and Perrichot, V., “Echoes from the cretaceous: new fossils shed light on the evolution of host detection and concealed ovipositor apparatus in the parasitoid wasp superfamily *orussoidea* (hymenoptera),” *Zoological Journal of the Linnean Society* **zlae021** (2024).
- [15] Brazidec, M., Vilhelmsen, L., Boudinot, B. E., Richter, A., Hammel, J. U., Perkovsky, E. E., Fan, Y., Wang, Z., Wu, Q., Wang, B., and Perrichot, V., “Unveiling ancient diversity of long-tailed wasps (hymenoptera: Megalyridae): new taxa from cretaceous kachin and taimyr ambers and their phylogenetic affinities,” *Arthropod Systematics and Phylogeny* **82**, 151–181 (2024).
- [16] Viertler, A., Verheyde, F., Schwarz, M., Schulz, G., Klopstein, S., and Menecart, B., “Three taphonomic stories of three new fossil species of darwin wasps (hymenoptera, ichneumonidae),” *Scientific Reports* **14**, 17415 (2024).
- [17] Ravichandran, N. K., Wijesinghe, R. E., Lee, S.-Y., Choi, K. S., Jeon, M., Jung, H.-Y., and Kim, J., “Non-destructive analysis of the internal anatomical structures of mosquito specimens using optical coherence tomography,” *Sensors* **17**, 1897 (2017).
- [18] Stavenga, D. G., Kruizinga, R., and Leertouwer, H. L., “Dioptrics of the facet lenses of male blowflies *calliphora* and *chrysomyia*,” *Journal of Comparative Physiology A* **166**, 365–371 (1990).
- [19] Land, M. F., Gibson, G., Horwood, J., and Zeil, J., “Fundamental differences in the optical structure of the eyes of nocturnal and diurnal mosquitoes,” *Journal of Comparative Physiology A* **185**, 91–103 (1999).
- [20] Choo, Y.-M., Buss, G. K., Tan, K., and Leal, W. S., “Multitasking roles of mosquito labrum in oviposition and blood feeding,” *Frontiers in Physiology* **6**, 306 (2015).
- [21] Winzeler, E. A., “Malaria research in the post-genomic era,” *Nature* **455**, 751–756 (2008).